

# Oligomannuronate prevents mitochondrial dysfunction induced by IAPP in RINm5F islet cells by inhibition of JNK activation and cell apoptosis

Qiong Li<sup>1,2</sup>, Xi Liu<sup>1,2</sup>, Xiaolei Cheng<sup>3,4</sup>, Zhichun Liu<sup>1,2</sup>, Xiaoliang Zhao<sup>3,4</sup>, Shuai Zhang<sup>1,2</sup>, Guangli Yu<sup>1,2</sup>, Xia Zhao<sup>1,2</sup>\*, Jiejie Hao<sup>1,2</sup>\*

<sup>1</sup>U1a Laboratory for Marine Drugs and Bioproducts, Qingdao National Laboratory for Marine Science and Technology, Qingdao 266237, China

<sup>2</sup>School of Medicine and Pharmacy, Ocean University of China, Qingdao 266003, China

<sup>3</sup>School of Life Science and Engineering, Lanzhou University of Technology, Lanzhou 730050, China

<sup>4</sup>The Affiliated Central Hospital of Qindao University, Qingdao 266001, China

**Corresponding Author:** Jiejie Hao, School of Medicine and Pharmacy, Ocean University of China, Qingdao 266003, China.

**Received:** July 03, 2019; **Accepted:** August 21, 2019; **Published:** August 27, 2019

## Abstract

Oligomannuronates (OM) are natural products from alginate that is frequently used as food supplement. The aim of this study was to investigate the in vitro protective effects of OM on RINm5F cells against human Islet amyloid polypeptide (IAPP) induced mitochondrial dysfunction, as well as the underlying mechanisms. Our results demonstrated that human IAPP induced mitochondrial dysfunction, as evidence by loss of  $\Delta\Psi_m$  and ATP content, and decrease in oxygen consumption and complex activities, was accompanied by JNK activation, changes in the expressions of Bcl-2 and Bax proteins, release of cytochrome c (Cyto-c) and apoptosis inducing factor (AIF) from mitochondria into cytosol. Interestingly, the human IAPP induced damage in RINm5F cells were effectively restored by co-treatment of OM. Moreover, JNK activation was required for the OM mediated changes in RINm5F cells. Taken together, our results suggested that OM prevented mitochondrial dysfunction induced by human IAPP in RINm5F islet cells through JNK dependent signaling pathways, suggesting a potential therapeutic role for OM in type 2 diabetes.

## Keywords

Oligomannuronate; Type 2 diabetes; Islet amyloid polypeptide; JNK activation; Mitochondrial dysfunction; RINm5F cells.

## Introduction

Islet formation is a pathological hallmark of type 2 diabetes occurring in the majority of patients [1,2], and is associated with decrease beta cell mass and function. Islet amyloid polypeptide (IAPP), or amylin, is a major component of the amyloid deposits. Human IAPP (hIAPP) is a 37 residue, natively unstructured peptide hormone that is co-stored and co-secreted from the beta cell secretory granules of the pancreatic islets [1,3]. hIAPP, unlike rat IAPP, contains critical structure for  $\beta$ -plated sheet formation and has propensity to aggregate and form amyloid fibrils [4]. Islet amyloid deposits have been associated with progressive loss of insulin-producing pancreatic beta cells mass in type 2 diabetic patients. In addition, synthetic hIAPP fibrils or oligomers induced apoptosis in both human and rat islet beta cells. In hIAPP transgenic mice models, increasing amyloid formation is linked to decreased beta cell mass and hyperglycemia [5,6]. Accumulating evidence indicates that cytotoxicity of hIAPP involves membrane disruption, endoplasmic reticulum stress, oxidative stress and mitochondrial dysfunction [5,7].

It is well known that mitochondria play a central role in the maintenance of energy store, regulation of metabolism and pathways of cell death. Previous studies suggested that metabolic dysregulation and insulin secretory failure might be due to mitochondrial dysfunction in the pathogenesis of type 2 diabetes [8,9]. Moreover, mitochondria participate in the control of islet beta cell mass. Several reports demonstrated that apoptosis due to mitochondrial dysfunction was especially apparent in pancreatic beta cells [7,10,11]. Besides, another central pathway to regulate beta cell growth and apoptosis is the c-Jun N-terminal protein kinase (JNK) pathway, which is activated in response to several stress stimuli, such as high glucose [12], ER stress [13,14], and hIAPP [15-17]. Recent investigations on the interplay between JNK pathway and mitochondria is focused on, and results revealed that the functional interactions of JNK and mitochondria is complicated and remains to be built up [18-22, 55-57], and moreover, the link between mitochondria function and JNK pathway in hIAPP-induced beta cell has not been reported.

Alginate, is a kind of acidic linear polysaccharide which consists of  $\beta$ -D-mannuronic acid and  $\alpha$ -L-guluronic acid [23]. Alginate

oligosaccharide and their derivatives have been widely used in the food, cosmetics and pharmaceutical industries [23,24]. Recently, low molecular weight alginate has attracted lots of scientific interest due to their bioactivity of plant growth promotion [25], anti-tumor [26,27], and neuron protection [28,29]. Moreover, some alginate-derived OM showed an outstanding activity in glucose and lipid metabolism in C2C12 skeletal muscle cells [30]. But there is no detailed information about the effects of OM on the pancreatic beta cells, no mention the comparative research in the relationship between the effects and OM with different molecular masses.

In the present study, we obtained several different molecular weights of OM, and then used the model of mitochondrial dysfunction induced by human IAPP in RINm5F islet cells to elucidate the role of JNK signaling pathway in human IAPP-induced islet  $\beta$ -cell mitochondrial dysfunction. As well as demonstrating the protective effects of OM, it is related to its ability to attenuate mitochondrial dysfunction.

## Materials and Methods

### Materials and reagents

Polymannuronic acid (M-block) with weight-average Molecular Weight (Mw) of 21.0 kDa was provided by Lantai Pharmaceutical Company (Qingdao, China). RPMI1640 medium, fetal bovine serum (FBS), penicillin, and streptomycin were purchased from Gibco (Grand Island, NY). Anti-phospho JNK (#4668), anti-Cyto c (#4280), anti-Bax (#5023), anti-Bcl 2(#3498) and anti-AIF (#5318) were from Cell Signaling Technology; other chemicals that were not specifically mentioned here were purchased from Sigma.

### Preparation of OMs and analytical methods

M-block was dissolved with dilute ammonia water in a Pyrex tube (pH=5) and hydrolyzed under microwave irradiation (1600 W, CEM corporation, Matthews, North Carolina, USA) at different conditions as previously described [31]. Four OMs were prepared at 2% (w/v), 130 °C, 20 min; 5 % (w/v), 120 °C, 5 min; 5 % (w/v), 100 °C, 20 min and 8 % (w/v), 100 °C, 10 min, respectively. The hydrolysates were decolorized by activated carbon and filtered by 0.22  $\mu$ m cellulose membrane, then freeze-dried to obtain OMs with different Mw compounds.

The relative weight-averaged Molecular Weight (Mw) of OMs made by microwave degradation were determined by high performance gel permeation chromatography combined with multi-angle laser light scattering (HPGPC-MALLS) on an Agilent 1260 chromatographic instrument. The OMs were dissolved in 0.1 mol/L Na<sub>2</sub>SO<sub>4</sub> elution solvent at a concentration of 5 mg/mL. Then 100  $\mu$ L of the sample was applied to a TSK gel G3000PWXL column (7.8 mm $\times$ 300 mm, Tosoh, Japan) with a flow rate of 0.6 mL/min. The temperature of column was maintained at 35 °C and the signal was detected by G1362A Refractive Index Detector (RID) and MALLS (Dawn Heleos-II, Wyatt technologies, USA). The Mw of each sample was calculated by Astra 5.3.4.20 software.

The total sugar content of OMs was determined according to the method of Dubois et al. using D-glucuronic acid as the standard [32]. The amount of uronic acids was determined using the carbazole reaction method described by Bitter and Muir, and D-glucuronic acid was used as the standard [33].

### Infrared spectral and NMR analysis

For FTIR analysis, the dried samples (1-2 mg) were mixed with 100 mg dried KBr and pressed to a transparent pellet and then analyzed with a Nicolet Nexus 470 FTIR spectrometer (Thermo Electron) under dry air at 400-4000 cm<sup>-1</sup>. And For <sup>1</sup>H-NMR and <sup>13</sup>C-NMR analyses, the sample was dissolved in D<sub>2</sub>O (99.96%) and freeze-dried twice to replace all exchangeable protons with deuterium. Spectra were acquired at 25 °C using JNM-ECP 600 MHz equipment (JNM-ECP 600, Jeol, Japan). Chemical shift values were calibrated using acetone-d<sub>6</sub> as an internal standard. The data were processed using the MestReNova software.

### Cell culture and treatments

RINm5F cells, from American Type Culture Collection (ATCC), were cultured in RPMI 1640 medium supplemented with 10% (v/v) fetal bovine serum, 2 mM L-glutamine, 100 U/mL penicillin, and 100  $\mu$ g/mL streptomycin, at 37 °C in a humidified (5% CO<sub>2</sub>, 95% air) atmosphere. All experiments were performed using cells between passages 21 and 30.

For peptide treatment, lyophilized hIAPP (Calbiochem) was dissolved in 80% hexafluoroisopropanol (HFIP, Sigma-Aldrich) to a concentration of 521  $\mu$ M, filtered over 0.2  $\mu$ m filters (Millipore), and stored at -20 °C until use. hIAPP aggregates were prepared by diluting hIAPP to 6.5  $\mu$ M in 10 mM phosphate buffer, pH7.4, 1.0% HFIP, and by incubating the mixture at 25 °C for 30 min before use.

Cells were pre-incubated with various concentrations of OMs for 48 h, and then remove the OMs and change for the fresh medium. Meanwhile, the hIAPP aggregates solution was applied to cultured cells at a final concentration of 250 nM for 24 h.

### MTT assay

RINm5F cells seeded in 96-well microplate were cultured at 37 °C in a humidified atmosphere for 72 h, and then the cells were exposed to different treatments for different periods of time. After incubation, 20  $\mu$ L/well of MTT solution (5 mg/mL in PBS buffer) was added and incubated for 4 h. The medium was aspirated and replaced with DMSO to dissolve the formazan salt. The color intensity of the formazan solution, which reflects the cell growth condition, was measured at 570 nm using a microplate spectrophotometer.

### Measurement of Mitochondrial Membrane Potential (MMP, $\Delta\Psi_m$ )

Determination of  $\Delta\Psi_m$  was carried out using the ratiometric dye JC-1 (5,5',6,6'-tetrachloro-1,1',3,3'-tetraethyl-benzimidazolyl-carbocyanine iodide), which is a dual emission potential-sensitive probe [34]. Freshly prepared cells were incubated with 10  $\mu$ g/mL of JC-1 for 30 min at 37 °C, washed twice with PBS, and then analyzed by a dual-wavelength/double-beam recording

spectrophotometer (Ex490nm, Em530 and Ex525nm, Em590).  $\Delta\Psi_m = A_{525} - A_{590} / A_{490} - A_{530}$  (Flex Station384, Molecular Devices, USA).

### Detection of intracellular Reactive Oxygen Species (ROS)

The production of cellular ROS was measured by 2',7'-dichlorofluorescein diacetate (DCFH2-DA) oxidation [35]. Freshly prepared cells were incubated with 2  $\mu$ M DCFH2-DA for 30 min at 37 °C, and then washed with PBS buffer, and the fluorescence was measured at 485 nm excitation and 535 nm emission recording spectrophotometer (Flex Station 384, Molecular Devices, USA).

### Determination of ATP content

The intracellular ATP content was determined using a bioluminescence somatic cell assay kit according to the manufacturer's instructions. After various treatments, cells were lysed by 0.5% Triton X-100 in 100 mM glycine buffer, pH 7.4. Intracellular ATP levels were assayed with an ATP bioluminescence assay kit (Sigma) based on the luciferase-catalyzed oxidation of D-luciferin [36]. The number of viable cells was counted with trypan blue using a hemacytometer. ATP level was expressed as femtomoles per cell.

### Mitochondrial respiration

Oxygen consumption by intact cells was measured as described [37]. After treatment, the islet beta cells were washed in KRH buffer plus 1% BSA. Cells from each condition were divided into triplicate aliquots and measured in a BD Oxygen Biosensor System plate (BD Biosciences). Plates were sealed and 'read' on a fluorescence spectrometer (Molecular Probes, Eugene, OR, USA) at 1 min intervals for 60 min at an excitation wavelength of 485 nm and emission wavelength of 630 nm. We have used  $5 \times 10^5$  cells in the assay. The oxygen consumption rate of cells generally follows Michaelis-Menten kinetics with respect to oxygen concentration.  $V_{max}$  is the maximum consumption rate.

### Activity of mitochondrial complexes I, II and III

RINm5F cells were cultured in 100 mm plates and washed in PBS. Following addition of trypsin, the cells were pelleted by centrifugation at 300 g for 5 min at 4 °C. All of the subsequent steps were performed on ice. The resulting pellet was then resuspended in mitochondrial isolation buffer (215 mM mannitol, 75 mM sucrose, 0.1% BSA, 1 mM EGTA, 20 mM HEPES, pH 7.2) and homogenized on ice with a glass homogenizer. The mitochondria were then purified by differential centrifugation at 1300 g for 5 min to pellet unbroken cells and the nuclei. The supernatant fraction was then centrifuged at 13 000 g for 10 min to pellet the mitochondria. The pellet was resuspended in EGTA-free isolation buffer. Briefly, complex I activity was assayed by monitoring the decrease of NADH at 340 nm. Final concentration of mitochondrial protein was 30 mg/mL. Reaction was started by adding 200 mM NADH and scanned at 340 nm for 3 min. Rotenone (3 mM) was added into the reaction system as blank control. Complex II was assayed with mitochondria

(final concentration 30 mg/mL), and the reaction was started with 10 mM succinate and scanned at 600 nm for 2 min. Complex III activity was measured in a mixture containing 250 mM sucrose, 1 mM EDTA, 50 mM K phosphate, pH adjusted to 6.5 to reduce autooxidation of reduced coenzyme Q1 (CoQ1), 2 mM KCN, 50 mM Cyto-c, 0.1% BSA, and the reaction was initiated by 20 mg/mL mitochondria and 50 mM reduced CoQ1, recording the increase of absorption at 550 nm for 2 min [38].

### Western blot analysis

To obtain cytosolic and mitochondrial fractions, the cells were incubated with buffer (20 mM Hepes, 1 mM EDTA, 10 mM KCl, 1.5 mM MgCl<sub>2</sub>, 1 mM EGTA, 1 mM dithiothreitol, 250 mM sucrose, aprotinin, leupeptin and pepstatin 2 mg/mL each, pH7.5) on ice for 30 min. After the cells were disrupted in a glass dounce homogenizer by optimized gentle strokes, homogenates were centrifuged at 1000 g for 10 min at 4 °C to remove nuclei. The supernatant was further centrifuged at 12000 g at 4 °C for 30 min to separate the mitochondria and cytosol fractions. To prepare whole cell lysates, the cells were harvested and incubated with lysis buffer by vortex. After centrifugation at 13000 g at 4 °C for 30 min to separate the cellular debris, the supernatant was collected and stored at -80 °C until use. The protein concentrations were determined using BCA protein assay kit according to the manufacturer's instructions.

Cell lysates (10 mg protein per lane) were subjected to 10% SDS-PAGE, then transferred to nitrocellulose membranes and blocked with 5% non-fat milk/Tris-buffered saline with Tween (TBST) for 1 h at room temperature. Membranes were incubated with primary antibodies directed against  $\beta$ -actin (1:10 000), p-JNK, Bax, cyto-C Bax, Bcl 2 and AIF in 5% milk/TBST at 4 °C overnight. After washing with TBST three times, membranes were incubated with horseradish peroxidase-conjugated secondary antibody for 1 h at room temperature. Western blots were developed using ECL (Roche Mannheim, Germany) and quantified by scanning densitometry [39]. Relative protein expressions determined by Western blotting were normalized to  $\beta$ -actin expression. Results were presented as percent control.

### Statistics

All values are expressed as means  $\pm$  S.E.M. Statistical significance was determined by using one-way ANOVA with Bonferroni's post hoc tests between the two groups. The criterion for significance was set at  $P < 0.05$ .

## Results

### Characterization of OMs

The Mw of OMs was 1678 Da for OM1.5, 3317 Da for OM3.0, 3910 Da for OM4.0, 5266 Da for OM5.0, respectively (Table 1). And the FT-IR spectrums of OMs are shown in (Figure 1A). The data revealed the bands at around 3398  $\text{cm}^{-1}$  were assigned to symmetric stretching vibration of the hydroxyl

group. The band at around 1729  $\text{cm}^{-1}$  was attributed to C=O stretching of carboxyl. The asymmetric and symmetric stretching of carboxylate vibrations appeared at 1610  $\text{cm}^{-1}$  and 1414  $\text{cm}^{-1}$ . The band at around 1098  $\text{cm}^{-1}$  (C-O-C stretching) and 1039  $\text{cm}^{-1}$  (C-O stretching) were the characteristic absorption bands of polysaccharide structure. The band at around 934  $\text{cm}^{-1}$  was the characteristic asymmetric stretching vibration of pyranose rings. The bands appeared at 816  $\text{cm}^{-1}$  were mannopyranuronic acid. Therefore, the products obtained from depolymeration of the PM remained mannuronate structure.

The structures of MOs were further characterized by NMR spectroscopy. To take OM3.0 as an example, the chemical shifts of anomeric protons were assigned according to  $^1\text{H}$ -NMR spectrum. As shown in (Figure. 1B), the apparent single peak at 5.22 ppm and double peak at 4.91-4.94 ppm corresponded to the reducing-end H1 and H1 $\beta$  signals respectively. The signal at 4.77 ppm was observed for the middle ring C1 H signal. The peak at 4.65 ppm was seen for the C1 proton of non-reducing-end. The signals between 3.6 ppm and 4.0 ppm were assigned to H2, H3, H4 and H5 of the reducing end, middle residue and non-reducing end. The 600 MHz  $^{13}\text{C}$  NMR spectra of OM3.0 are given in (Figure. 1C). Chemical shifts were unambiguously assigned. A single peak at 175.49-176.23 ppm was seen for the C6 of pyranose rings. The peak at around 94 ppm corresponded to the C1 signals of the reducing end. Peaks at 101.51 ppm and 100.05 ppm were assigned to C1 of non-reducing end and the middle ring, respectively. The signal appeared at 77.75 ppm was assigned to C4r and C4m. The signal appeared at 75.84 ppm was seen for the C4n/C5r $\beta$ /C5m. The peak at 72.72 ppm was assigned to the resonance of C5n. The signals appeared around 69-72 ppm was attributed to C3 and C2 of pyranose rings, respectively.

### Cell toxicities of OMs

As shown in (Figure. 2.), treatment of RINm5F cells with different concentrations of OMs indicated as OM1.5, OM3.0, OM4.0, OM5.0, tended to increase the cell viability determined by MTT method, which demonstrated that OMs had no toxic effect on RINm5F cells within the ranged concentrations of 0-250  $\mu\text{M}$ , and these results were in line with our previous report in C2C12 skeletal muscle cells [30]. Meanwhile, the OM3.0 treatment could significantly increase the cell viability of RINm5F cells at levels of 50-250  $\mu\text{M}$ . In addition, there was no obvious increase in the MTT assay of RINm5F cells induced with OMs at the concentration of 250  $\mu\text{M}$  as compared with 50  $\mu\text{M}$ . So, we choose the 10 and 50  $\mu\text{M}$  to continue our  $\Delta\Psi\text{m}$  detection.

**Table 1** The relative weight-average molecular weight ( $M_w$ ), total sugar content and uronic acid content of OMs.

Samples	$M_w$ (Da)	D	Total sugar (%)	Uronic acid (%)
OM1.5	1678	1.02	93.27 $\pm$ 1.39	88.58 $\pm$ 1.88
OM3.0	3317	1.21	93.47 $\pm$ 0.80	88.83 $\pm$ 0.92
OM4.0	3910	1.34	94.21 $\pm$ 1.64	91.46 $\pm$ 0.93
OM5.0	5266	1.4	95.17 $\pm$ 2.46	93.28 $\pm$ 1.08

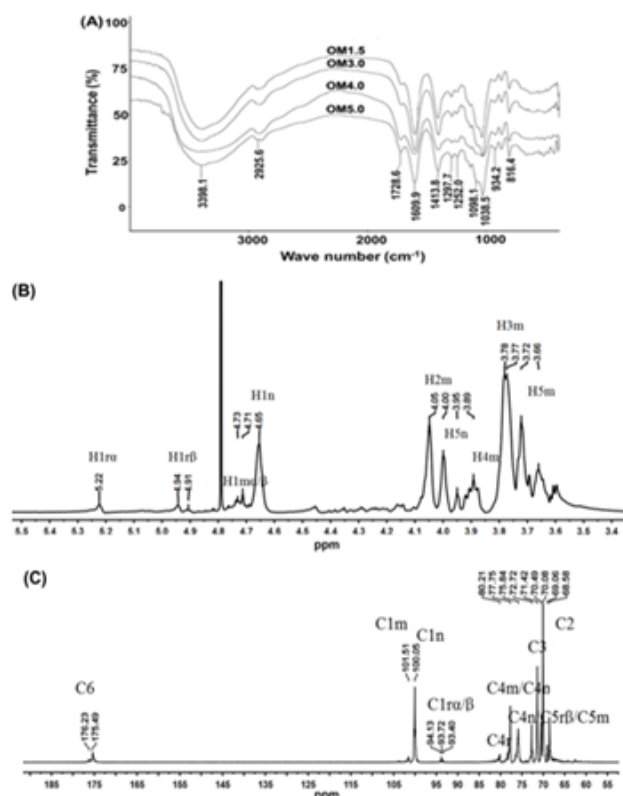


**Figure 1.** The FTIR and  $^1\text{D}$ -NMR analysis. (A) FTIR spectrum of OMs. (B)  $^1\text{H}$ -NMR spectrum of OM3.0. (C)  $^{13}\text{C}$ -NMR spectrum of OM3.0.

### Effect of OMs on mitochondrial membrane potential (MMP)

As shown in (Figure. 3A.), pre-treatment of RINm5F cells with OMs at different concentrations as indicated could obviously inhibit the reductions of  $\Delta\Psi\text{m}$  in RINm5F cells induced by IAPP as determined by JC-1 assay. And among the OMs with different molecular weights from 1.5 kDa to 5.0 kDa, the OM3.0 with molecular weight of 3.0 kDa tends to be the best one. Meanwhile, in the absence of IAPP addition, OMs had no effect on RINm5F cells within the ranged concentrations of 10-50  $\mu\text{M}$ .

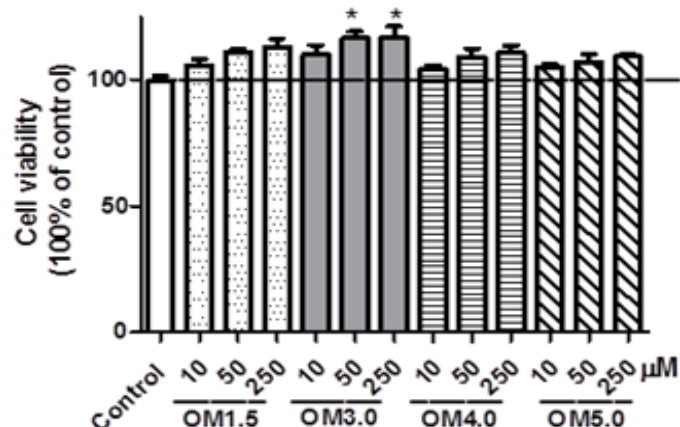


**Figure 2.** The cytotoxicities of OMs on RINm5F cells. Cells were incubated with indicated OMs at indicated concentrations for 72 h. The cell viability was evaluated by MTT assay as described in materials and methods. Values are means  $\pm$  S.E.M of four replicates. \* $P < 0.05$  versus the IAPP model.



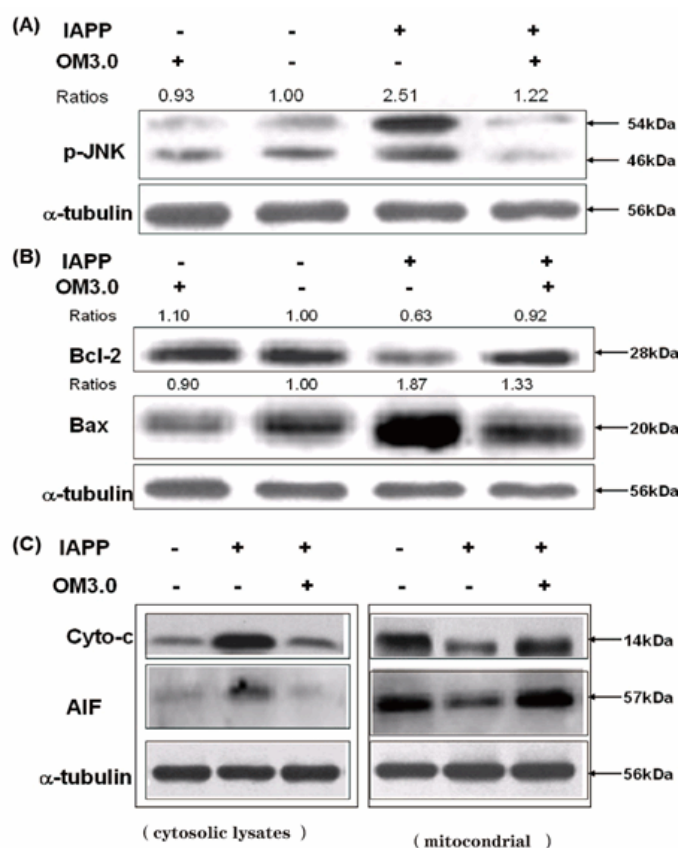
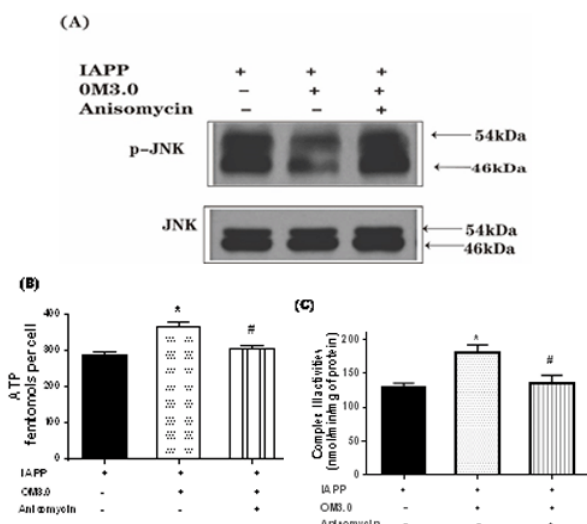


**Figure 5.** OM<sub>3.0</sub> suppressed JNK activation and cell apoptosis in IAPP induced islet  $\beta$  cells. RINm5F cells in 6-well plates were treated with OMs at 50  $\mu$ M for 48 h, and then induced with IAPP (250 nM) for 24 h. "No IAPP was added and no OM<sub>3.0</sub> was added" as a control group. (A) Inhibition of JNK activation by OM<sub>3.0</sub> treatment. Cell lysates were subjected to western blot analysis of phosphorylated JNK.  $\alpha$ -tubulin was used as an internal control. (B) Effect of OM<sub>3.0</sub> on protein expression of Bcl-2 and Bax. Cell lysates were subjected to western blot analysis of Bcl-2 and Bax,  $\alpha$ -tubulin was used as an internal control. (C) OM<sub>3.0</sub> prevented IAPP induced changes of Cyto-c and AIF release from mitochondria into cytosol. The treated cells were separated into cytosolic and mitochondrial fractions. Cell lysates were subjected to western blot analysis. Changes in levels of protein expression (shown as ratios) were calculated based on levels in corresponding untreated cells, which were set at unity. Data represent similar results from three independent experiments.



time that mitochondrial dysfunction induced by hIAPP was dependent on the JNK signaling pathway in pancreatic beta cells. Our results showed that disruption of mitochondrial function in hIAPP induced RINm5F cell, as evidence by loss of MMP, suppressed mitochondrial complex activities, ATP depletion, decreased respiratory consumption, elevated apoptotic protein expression and Cyto-c release, was mediated by the JNK activation. Interestingly, these hIAPP-induced changes were significantly attenuated by OMs treatments, which were partially due to its ability to prevent mitochondrial dysfunction through a JNK mediated signaling pathway.

Recent years, lot of poly-/oligosaccharides have been investigated and showed anti-diabetic activities, for example, hypoglycemic activities have been revealed for chito-oligosaccharides, and oligosaccharides from two kinds of fungi [41-44,58-62]. But no information about the beneficial effect of OMs on the hIAPP-induced pancreatic beta cells. Due to the commercially wide use of OMs, we obtained several kinds of OMs with different molecular mass by microwave degradation, and compared their protective effects on the MMP loss induced by hIAPP in RINm5F cells. In the present work, several water-soluble OMs were prepared by microwave-irradiation method. The molecular weights of OMs were about 1.5-5.0 kDa, as determined by HPGPC-MALLS. And the results showed that OMs, especially for the molecular weight of 3.0 kDa, could effectively inhibit the MMP loss in hIAPP-treated RINm5F cells. In our previous study, we also found that the OM-derived chromium (III) complexes with the molecular weight of around 3.0 kDa significantly stimulated insulin sensitivity in C2C12 skeletal muscles [30]. These data demonstrated an optimized concentration of OM around 3.0 kDa to exert its bioactivity on skeletal or pancreatic islet beta cells, which could share some insight for its potential in industrial applications.

The mitochondrion of pancreatic beta cell is a key organelle for control of insulin secretion. Several published studies revealed that beta cell apoptosis due to mitochondrial dysfunction was especially apparent in pancreatic beta cells [8,9]. The mitochondrial respiratory chain is a major source of ROS whose over-production of ROS will further impair mitochondrial electron transport to cause more ROS release. ROS has been highlighted as initiators for hIAPP-induced cytotoxicity in pancreatic beta cells. Previous findings suggested that over-production of ROS was involved in hIAPP-induced beta cell toxicity [1,13,45]. Moreover, ROS are known to affect MMP, and the loss of MMP induces release of mitochondrial apoptogenic factors, such as Cyto-c and AIF [10,11]. Once in the cytol, Cyto-c binds to adaptor molecule apoptotic protease activating factor I (Apaf-1) in the presence of ATP and activates caspase-9, which in turn activates caspase-3 and cleaves downstream PARP, and eventually leads to cell apoptosis [46]. In contrast to Cyto-c, AIF mediated the apoptotic cell death through a caspase-independent pathway [47]. In the present study, we found that hIAPP treatment induced intracellular ROS generation in RINm5F cells accompanied with damages in mitochondrial function, including loss of MMP, depletion of ATP, release of apoptogenic factors such as Cyto-c and AIF, increased expression of Bax, and decreased expression Bcl-2, which was attenuated by co-treatment with OMs. Meanwhile, the JNK activation and downstream targets

were also down-regulated by OMs treatments in pancreatic beta cells. These results suggest that OM is capable of scavenging free radicals and protects RINm5F cells against hIAPP-induced mitochondrial damage, which was associated with the activation of JNK signaling pathway.

JNK signaling has an established role in the regulation of cell apoptosis through the activation of transcription factors and phosphorylation of apoptosis-related proteins [40,48,49]. The JNK signaling pathway has been reported to affect members of the Bcl-2 family. For example, JNK not only can inactivate anti-apoptotic Bcl-2 proteins but also can activate the mitochondrial translocation of Bax [50]. But conversely, there is growing evidence that JNK signaling can induce pro-survival pathways in certain cell types, including neurons, T cells and B lymphocytes [51,52]. Thus, the role of JNK is complex in the mediation of distinct cellular response depending on cell contents. In addition, different concentrations of hIAPP could result in different cellular responses, for example, the activation of NADPH-oxidase induced by hIAPP at 60 nM was converse to the concentration at 500 nM [53]. And recent researches were focused on the molecular or signal changes induced by hIAPP at  $\mu\text{M}$  levels [1,6,7,16,40,54]. And in RINm5F cells, activation of JNK was associated with hIAPP-induced cell damage [15,54]. In the present study, we firstly found that hIAPP at 250 nM could effectively stimulate the activation of JNK in RINm5F cells. In support of the pro-apoptosis functions of JNK in the presence of hIAPP, our results also demonstrated that the protective effects of OM on beta cells were partially mediated by suppressing the activation of JNK pathway.

The signal interactions of JNK with mitochondria were complicated as reported [18-22], in the present study, we demonstrated for the first time that the mitochondrial dysfunction induced by hIAPP was dependent on the activation of JNK. Meanwhile, the stimulation of JNK by specific activators also obviously abrogated the beneficial effect of OM on the hIAPP-induced mitochondrial damage in RINm5F cells, indicating the prevention of mitochondrial damage in IAPP-treated RINm5F islet cells by OM treatment was through a JNK dependent signaling pathway.

## Conclusions

In this study, our results provide strong evidence that hIAPP-induced mitochondrial dysfunction in RINm5F islet beta cells through was through activation of JNK signaling pathway. Moreover, treatment with OM effectively attenuated hIAPP-induced loss of MMP, ATP depletion, reduced mitochondrial complex activities, decreased Bcl-2, increased Bax levels protein and release of Cyto-c, these effects were in part mediated by the activation of JNK. The present work enhances our understanding of the molecular mechanisms of hIAPP-induced pancreatic mitochondrial dysfunction and indicates the potential therapeutic role of OM in type 2 diabetes by preventing hIAPP-induced loss of pancreatic beta cells.

## Acknowledgements

This research was supported by National Science Foundation of China (81402982), NSFC-Shandong Joint Fund for Marine Science Research Center (U1406402), and Qingdao Independent

Innovation Project (13-7-1-zdxx1-hy).

## Conflicts of Interest

The authors declare no conflict of interest.

## References

- Zraika, S., Hull, R. L., Udayasankar, J., Aston-Mourney, K., Subramanian, et al. (2009). Oxidative stress is induced by islet amyloid formation and time-dependently mediates amyloid-induced beta cell apoptosis. *Diabetologia*. 56:626-635. [[Crossref](#)].
- Westermarck, P., Wernstedt, C., Wilander, E., Hayden, D. W., O'Brien, T. D., et al. (1987). Amyloid fibrils in human insulinoma and islets of Langerhans of the diabetic cat are derived from a neuropeptide-like protein also present in normal islet cells. *Proceedings of the National Academy of Sciences of the United States of America*. 84:3881-3885. [[Crossref](#)].
- Cao, P., Marek, P., Noor, H., Patsalo, Tu L. H., et al. (2013). Islet amyloid: from fundamental biophysics to mechanisms of cytotoxicity. *FEBS Letters*. 587:1106-1118. [[Crossref](#)].
- Haataja, L., Gurlo, T., Huang, C. J., & Butler, P. C. (2008). Islet amyloid in type 2 diabetes, and the toxic oligomer hypothesis. *Endocrine Reviews*. 29:303-316. [[Crossref](#)].
- Hoppener, J. W. M., & Lips, C. J. M. (2006). Role of islet amyloid in type 2 diabetes mellitus. *The International*. 38:726-736. [[Crossref](#)].
- Lin, C. Y., Gurlo, T., Kayed, R., Butler, A. E., Haataja, L. et al. (2007). Toxic human islet amyloid polypeptide (h-IAPP) oligomers are intracellular, and vaccination to induce anti-toxic oligomer antibodies does not prevent h-IAPP-induced beta-cell apoptosis in h-IAPP transgenic mice. *Diabetes*. 56:1324-1332. [[Crossref](#)].
- Li, X., Chen, T., Wong, Y., Xu G., Fan, R., et al. (2011). Involvement of mitochondrial dysfunction in human islet amyloid polypeptide-induced apoptosis in INS-1E pancreatic beta cells: An effect attenuated by phycocyanin. *The International Journal of Biochemistry & Cell Biology*. 43:525-534. [[Crossref](#)].
- Trifunovic, A., & Larsson, N. G. (2008). Mitochondrial dysfunction as a cause of ageing. *Journal of Internal Medicine*. 263:167-178. [[Crossref](#)].
- Butler, A. E., Janson, J., Bonner-Weir, S., Ritzel, R., Rizza, R. A., et al. (2003). Beta-cell deficit and increased beta-cell apoptosis in humans with type 2 diabetes. *Diabetes*. 52:102-110. [[Crossref](#)].
- Gupta, S., Kass, G. E. N., Szegezdi, E., & Joseph, B. (2009). The mitochondrial death pathway: a promising therapeutic target in diseases. *Journal of Cellular and Molecular Medicine*. 13:1004-1033. [[Crossref](#)].
- Jourdain, A., & Martinou, J. C. (2009). Mitochondrial outer-membrane permeabilization and remodeling in apopto-

- sis. *The International Journal of Biochemistry & Cell Biology*. 41:1884-1889. [[Crossref](#)].
12. Maedler, K., Schulthess, F. T., Bielman, C., Berney, T., Bonny, C., et al. (2008). Glucose and leptin induce apoptosis in human beta-cells and impair glucose-stimulated insulin secretion through activation of c-Jun N-terminal kinases. *FASEB Journal*. 22:1905-1913. [[Crossref](#)].
  13. Kaneto, H., Matsuoka, T. A., Nakatani, Y., Kawamori, D., Miyatsuka, T., et al. (2005). Oxidative stress, ER stress, and the JNK pathway in type 2 diabetes. *Journal of Molecular Medicine (Berlin, Germany)*. 83:429-439. [[Crossref](#)].
  14. Cunha, D. A., Hekerman, P., Ladriere, L., Bazarra-Castro, A., Ortis, F., et al. (2008). Initiation and execution of lipotoxic ER stress in pancreatic beta-cells. *Journal of Cell Science*. 121:2308-2318. [[Crossref](#)].
  15. Zhang, S., Liu, J., Dragunow, M., & Cooper, G. J. (2003). Fibrillogenic amylin evokes islet beta-cell apoptosis through linked activation of a caspase cascade and JNK1. *Journal of Biological Chemistry*. 278:52810-52819. [[Crossref](#)].
  16. Li, X., Xu, G., Chen, T., Wong, Y., Zhao, H., et al. (2009). Phycocyanin protects INS-1E pancreatic beta cells against human islet amyloid polypeptide-induced apoptosis through attenuating oxidative stress and modulating JNK and p38 mitogen-activated protein kinase pathways. *International Journal of Biochemistry & Cell Biology*. 41:1526-1535. [[Crossref](#)].
  17. Zhang, S., Liu, J., MacGibbon, G., Dragunow, M., & Cooper, G. J. (2002). Increased expression and activation of c-Jun contributes to human amylin-induced apoptosis in pancreatic islet beta-cells. *Journal of Molecular Biology*. 324:271-285. [[Crossref](#)].
  18. Dhanasekaran, D. N., & Reddy, E. P. (2008). JNK signaling in apoptosis. *Oncogene*. 27:6245-6251. [[Crossref](#)].
  19. Chambers, J. W., Pachori, A., Howard, S., Iqbal, S., & Lo-grasso, P. V. (2013). Inhibition of JNK mitochondrial localization and signaling is protective against ischemia/reperfusion injury in rats. *Journal of Biological Chemistry*. 288:4000-4011. [[Crossref](#)].
  20. Dougherty, C. J., Kubasiak, L. A., Frazier, D. P., Li, H., Xiong, W. C., et al. (2004). Mitochondrial signals initiate the activation of c-Jun N-terminal kinase (JNK) by hypoxia-reoxygenation. *FASEB Journal*. 18:1060-1070. [[Crossref](#)].
  21. Hanawa, N., Shinohara, M., Saberi, B., Gaarde, W. A., Han, D., et al. (2008). Role of JNK translocation to mitochondria leading to inhibition of mitochondria bioenergetics in acetaminophen-induced liver injury. *Journal of Biological Chemistry*. 283:13565-13577. [[Crossref](#)].
  22. Wang, L., Tu, Y., Huang, C., & Ho, C. (2012). JNK signaling is the shared pathway linking neuroinflammation, blood-brain barrier disruption, and oligodendroglial apoptosis in the white matter injury of the immature brain. *Journal of Neuroinflammation*. 9:175. [[Crossref](#)].
  23. Li, L., Jiang, X., Guan, H., & Wang, P. (2011). Preparation, purification and characterization of alginate oligosaccharides degraded by alginate lyase from *Pseudomonas* sp. HZJ 216. *Carbohydrate Research*. 346:794-800. [[Crossref](#)].
  24. Choi, D., Piao, Y. L., Shin, W. S., & Cho, H. (2009). Production of oligosaccharide from alginate using *Pseudoalteromonas agarovorans*. *Applied Biochemistry and Biotechnology*. 159:438-452. [[Crossref](#)].
  25. Natsume, M., Kamo, Y., Hirayama, M., & Adachi, T. (1994). Isolation and characterization of alginate-derived oligosaccharides with root growth-promoting activities. *Carbohydrate Research*. 258:187-197. [[Crossref](#)].
  26. Hu, J., Geng, M., Li, J., Xin, X., Wang, J., et al. (2004). Acidic oligosaccharide sugar chain, a marine-derived acidic oligosaccharide, inhibits the cytotoxicity and aggregation of amyloid beta protein. *Journal of Pharmacological Sciences*. 95:248-255. [[Crossref](#)].
  27. Ma, J., Xin, X., Meng, L., Tong, L., Lin, L., et al. (2008). The marine-derived oligosaccharide sulfate (MdOS), a novel multiple tyrosine kinase inhibitor, combats tumor angiogenesis both in vitro and in vivo. *PLoS One*, 3: e3774. [[Crossref](#)].
  28. Wang, X. J., Chen, X. H., Yang, X. Y., Geng, M. Y., & Wang, L. M. (2007). Acidic oligosaccharide sugar chain, a marine-derived oligosaccharide, activates human glial cell line-derived neurotrophic factor signaling. *Neuroscience Letters*. 417:176-180. [[Crossref](#)].
  29. Wang, S., Li, J., Xia, W., & Geng, M. (2007). A marine-derived acidic oligosaccharide sugar chain specifically inhibits neuronal cell injury mediated by beta-amyloid-induced astrocyte activation in vitro. *Neurological Research*. 29:96-102. [[Crossref](#)].
  30. Hao, C., Hao, J., Wang, W., Han, Z., Li, G., et al. (2011). Insulin sensitizing effects of oligomannuronate-chromium (III) complexes in C2C12 skeletal muscle cells. *PLoS One*. 6: e24598. [[Crossref](#)].
  31. Hu, T., Li, C., Zhao, X., Li, G., Yu, G., et al. (2013). Preparation and characterization of guluronic acid oligosaccharides degraded by a rapid microwave irradiation method. *Carbohydrate Research*. 373:53-58. [[Crossref](#)].
  32. Dubois, M., Gilles, K., Hamilton, J. K., Rebers, P. A., & Smith, F. (1951). A colorimetric method for the determination of sugars. *Nature*. 28:168, 167. [[Crossref](#)].
  33. Bitter, T., & Muir, H. M. (1962). A modified uronic acid carbazole reaction. *Analytical Biochemistry*. 4: 330-334. [[Crossref](#)].
  34. Tirosh, O., Sen, C. K., Roy, S., & Packer, L. (2000). Cellular and mitochondrial changes in glutamate-induced HT4 neuronal cell death. *Neuroscience*. 97:531-541. [[Crossref](#)].
  35. Cathcart, R., Schwieters, E., & Ames, B. N. (1983). Detection of picomole levels of hydroperoxides using a fluorescent dichlorofluorescein assay. *Analytical Biochemistry*. 134:111-116. [[Crossref](#)].
  36. Patane, G., Anello, M., Piro, S., Vigneri, R., Purrello, F., et al. (2002). Role of ATP production and uncoupling protein-2 in the insulin secretory defect induced by chronic

- exposure to high glucose or free fatty acids and effects of peroxisome proliferator-activated receptor-gamma inhibition. *Diabetes*. 51:2749-2756. [[Crossref](#)].
37. Wilson-Fritch, L., Nicoloso, S., Chouinard, M., Lazar, M. A., Chui, P. C., et al. (2004). Mitochondrial remodeling in adipose tissue associated with obesity and treatment with rosiglitazone. *Journal of Clinical Investigation*. 114:1281-1289. [[Crossref](#)].
  38. Sun, L., Luo, C., Long, J., Wei, D., & Liu, J. (2006). Acrolein is a mitochondrial toxin: effects on respiratory function and enzyme activities in isolated rat liver mitochondria. *Mitochondrion*. 6:136-142. [[Crossref](#)].
  39. Boudina, S., Sena, S., O'Neill, B. T., Tathireddy, P., Young, M. E., et al. (2005). Reduced mitochondrial oxidative capacity and increased mitochondrial uncoupling impair myocardial energetics in obesity. *Circulation*. 112:2686-2695. [[Crossref](#)].
  40. Subramanian, S. L., Hull, R. L., Zraika, S., Aston-Mourney, K., Udayasankar, J., et al. (2012). cJUN N-terminal kinase (JNK) activation mediates islet amyloid-induced beta cell apoptosis in cultured human islet amyloid polypeptide transgenic mouse islets. *Diabetologia*. 55:166-174. [[Crossref](#)].
  41. Zhang, R., Zhou, J., Jia, Z., Zhang, Y., & Gu, G. (2004). Hypoglycemic effect of *Rehmannia glutinosa* oligosaccharide in hyperglycemic and alloxan-induced diabetic rats and its mechanism. *Journal of Ethnopharmacology*. 90:39-43. [[Crossref](#)].
  42. Liu, B., Liu, W. S., Han, B. Q., & Sun, Y. Y. (2007). Anti-diabetic effects of chito-oligosaccharides
  43. on pancreatic islet cells in streptozotocin-induced diabetic rats. *World Journal of Gastroenterology*. 13:725-731. [[Crossref](#)].
  44. Lu, X. J., Chen, X. M., Fu, D. X., Cong, W., & Ouyang, F. (2002). Effect of *Amorphophallus konjac* oligosaccharides on STZ-induced diabetes model of isolated islets. *Life Sciences*. 72:711-719. [[Crossref](#)].
  45. Wang, X., Zheng, Y., & Fang, J. (2004). Recent advances in the study on poly- and oligo-saccharides with hypoglycemic activity. *Acta pharmaceutica Sinica*. 39:1028-1033. [[Crossref](#)].
  46. Konarkowska, B., Aitken, J. F., Kistler, J., Zhang, S., & Cooper, G. J. (2006). The aggregation potential of human amylin determines its cytotoxicity towards islet beta-cells. *FEBS Journal*. 273:3614-3624. [[Crossref](#)].
  47. Kroemer, G., & Reed, J. C. (2000). Mitochondrial control of cell death. *Nature Medicine*. 6:513-519. [[Crossref](#)].
  48. Krantic, S., Mechawar, N., Reix, S., & Quirion, R. (2007). Apoptosis-inducing factor: a matter of neuron life and death. *Progress in Neurobiology*. 81:179-196. [[Crossref](#)].
  49. Abdelli, S., Abderrahmani, A., Hering, B. J., Beckmann, J. S., & Bonny, C. (2007). The c-Jun N-terminal kinase JNK participates in cytokine- and isolation stress-induced rat pancreatic islet apoptosis. *Diabetologia*. 50: 1660-1669. [[Crossref](#)].
  50. Liu, G., & An, Z. (2009). Protective effect of rosiglitazone sodium on islet beta-cell of STZ induced diabetic rats through JNK pathway. *Journal of Sichuan University - Medical Science Edition*. 40:430-434. [[Crossref](#)].
  51. Lee, H., Wang, C., Kuo, H., Chou, F., Jean, L., et al. (2005). Induction apoptosis of luteolin in human hepatoma HepG2 cells involving mitochondria translocation of Bax/Bak and activation of JNK. *Toxicology and Applied Pharmacology*. 203:124-131. [[Crossref](#)].
  52. Liu, J., & Lin, A. (2005). Role of JNK activation in apoptosis: a double-edged sword. *Cell Research*. 15:36-42. [[Crossref](#)].
  53. Xu, L., Yu, J., Zhai, D., Zhang, D., Shen, W., et al. (2014). Role of JNK activation and mitochondrial Bax translocation in allicin-induced apoptosis in human ovarian cancer SKOV3 cells. *Evidence-based Complementary and Alternative Medicine*. 2014:378684. [[Crossref](#)].
  54. Borchi, E., Bargelli, V., Guidotti, V., Berti, A., Stefani, M., et al. (2014). Mild exposure of RIN-5F  $\beta$ -cells to human islet amyloid polypeptide aggregates upregulates antioxidant enzymes via NADPH oxidase-RAGE: an hormetic stimulus. *Redox Biology*. 2:114-122. [[Crossref](#)].
  55. Rumora, L., Hadzija, M., Barisic, K., Maysinger, D., & Grubiic, T. Z. (2002). Amylin-induced cytotoxicity is associated with activation of caspase-3 and MAP kinases. *Biological Chemistry*. 383:1751-1758. [[Crossref](#)].
  56. Geng, C., Wei, J., and Wu, C. (2019). Mammalian STE20-like Kinase 1 Knockdown Attenuates TNF $\alpha$ -Mediated Neurodegenerative Disease by Repressing the JNK Pathway and Mitochondrial Stress. *Neurochemical Research*. 44:1653-1664. [[Crossref](#)].
  57. Wu, Y.-J., Su, T.-R., Dai, G.-F., Su, J.-H., and Liu, C.-I. (2019). Flaccidoxide-13-Acetate-Induced Apoptosis in Human Bladder Cancer Cells is through Activation of p38/JNK, Mitochondrial Dysfunction, and Endoplasmic Reticulum Stress Regulated Pathway. *Marine drugs*. 17:pii-E287. [[Crossref](#)].
  58. Zhou, H., Wang, J., Hu, S., Zhu, H., Toan, S., et al. (2019). BII alleviates cardiac microvascular ischemia reperfusion injury via modifying mitochondrial fission and inhibiting XO/ROS/F-actin pathways. *Journal of cellular physiology*. 234:5056-5069. [[Crossref](#)].
  59. Sanger, G., Rarung, L., Damongilala, L., Kaseger, B., and Montolalu, L. (2019). Phytochemical constituents and anti-diabetic activity of edible marine red seaweed (*Halymenia durvillae*). In *IOP Conference Series: Earth and Environmental Science*. (IOP Publishing). 278:012069. [[Crossref](#)].
  60. Yang, C.-f., Lai, S.-s., Chen, Y.-h., Liu, D., Liu, B., et al. (2019). Anti-diabetic effect of oligosaccharides from seaweed *Sargassum confusum* via JNK-IRS1/PI3K signaling pathways and regulation of gut microbiota. *Food and Chemical Toxicology*. 131:110562. [[Crossref](#)].
  61. Wang, Z., Zhao, X., Liu, X., Lu, W., Jia, S., et al. (2019). An

- ti-diabetic activity evaluation of a polysaccharide extracted from *Gynostemma pentaphyllum*. *International journal of biological macromolecules*. 126:209-214. [[Crossref](#)].
62. Tao, X., Liang, S., Che, J.-Y., Li, H., Sun, H.-X., et al. (2019). Antidiabetic Activity of Acidic Polysaccharide From *Schisandra chinensis* in STZ-Induced Diabetic Mice. *Natural Product Communications*. 14:1934578X19850374. [[Crossref](#)].
63. Wang, X., Zhang, Z., Wu, Y., Sun, X., and Xu, N. (2019). Synthesized sulfated and acetylated derivatives of polysaccharide extracted from *Gracilariopsis lemaneiformis* and their potential antioxidant and immunological activity. *International journal of biological macromolecules*. 124:568-572. [[Crossref](#)].